

Supporting Information for

Cation-induced molecular motion of springlike [2]catenanes

Alexandre V. Leontiev, Christopher J. Serpell, Nicholas G. White, and Paul D. Beer

Department of Chemistry, Chemistry Research Laboratory, University of Oxford, Mansfield Road, Oxford, OX1 3TA

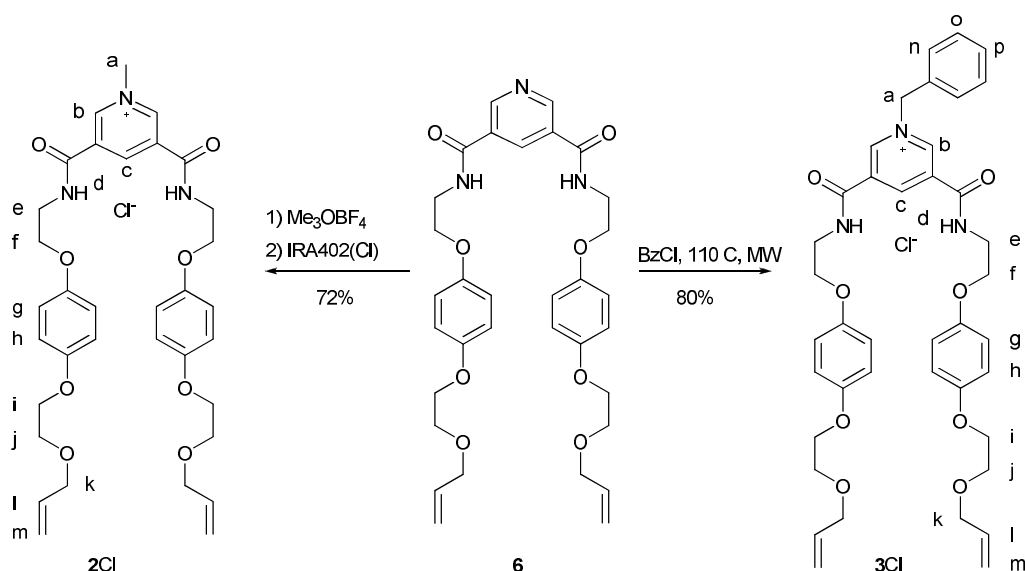
Synthesis of compounds 3Cl , 4Cl and 5Cl	S3
Anion exchange of 4Cl to 4PF₆ and 5Cl to 5PF₆	S5
¹ H and ROESY spectra of	
Compounds 1 , 2Cl and 4Cl	S6
Compounds 1 , 2PF₆ and 4PF₆	S7
Compounds 1 , 3Cl and 5Cl	S8
Compound 4Cl (ROESY)	S9
Compound 5Cl (NOESY)	S10
Compound 4PF₆ (ROESY)	S11
Compound 4Cl and 4PF₆	S12
Compounds 4PF₆ with NaClO ₄	S13
Compound 4PF₆ with Ba(ClO ₄) ₂	S14
Compound 4PF₆ with Ba(ClO ₄) ₂ (ROESY)	S15
UV-vis titrations of 5PF₆ with NaClO ₄	S16
¹ H NMR and UV vis titrations protocols	S16
Crystallographic data for	
Calixdiquinone macrocycle 1	S18
Benzyl [2]catenane 5Cl	S19
Methyl [2]catenane 4Cl	S20
References	S23

General considerations

All solvents and reagents were purchased from commercial suppliers and used as received unless otherwise stated. Dry solvents were obtained by purging with nitrogen and then passing through an MBraun MPSP-800 column. H₂O was de-ionised and micro filtered using a Milli-Q® Millipore machine. Et₃N was distilled and stored over KOH. TBA salts were stored in a vacuum desiccator containing phosphorus pentoxide prior to use. ¹H, ¹³C, ¹⁹F and ³¹P NMR spectra were recorded on a Varian Mercury-VX 300, a Varian Unity Plus 500 or a Bruker AVII500 with cryoprobe at 293 K. Chemical shifts are quoted in parts per million relative to the residual solvent peak. Mass spectra were obtained using a Micromass GCT (EI) instrument, a Micromass LCT (ESMS) instrument or a Maldi Micro MX instrument. Electronic absorption spectra were recorded on a PGT60 U spectrophotometer. Microwave reactions were carried out using a Biotage Initiator 2.0 microwave. Melting points were recorded on a Gallenkamp capillary melting point apparatus and are uncorrected.

Synthesis of catenane precursor 3Cl

The compound **1**, **2Cl** and **6** were prepared as described previously.^{1,2} The pyridinium thread **3Cl** was synthesised by alkylation of the precursor **6** with benzyl chloride according to the scheme below.



Scheme S1 Synthesis of pyridinium threads **2Cl** and **3Cl**.

Pyridinium thread 3Cl

The precursor **6** (0.15 g, 0.27 mmol) and benzyl chloride (0.66 g, 0.6 mL, 5 mmol) in 1 mL of dry acetonitrile were heated in the microwave at 110 °C for 2 hrs. The reaction mixture was then washed with hot hexane (5×2 mL) to remove excess of BzCl. Resulting gum-like residue was recrystallized from CHCl_3 /hexane to give the crude product. This was further purified using silica gel column chromatography (DCM/MeOH 9:1) to give the product as a yellow solid (0.144 g, 0.2 mmol, 80%); ^1H NMR (300 MHz, CDCl_3) δ (ppm) 10.16 (s, 1H), 9.61 (s, 2H), 9.58 (s, 2H), 7.40 (m, 5H), 6.69 (dd, $J = 25.6, 9.1$ Hz, 8H), 5.97 – 5.85 (m, 2H), 5.84 (s, 2H), 5.30 – 5.15 (m, 4H), 4.19 – 3.88 (m, 12H), 3.88 – 3.57 (m, 8H); ^{13}C NMR (75 MHz, CDCl_3) δ 160.6, 153.0, 152.7, 145.3, 142.1, 134.5, 134.1, 131.4, 130.6, 129.9, 129.4, 117.5, 115.7, 115.4, 72.3, 68.6, 67.9, 66.4, 65.6, 40.3; m/z (ESI-MS) $[\text{M} - \text{Cl}]^+$ 696.33, $\text{C}_{40}\text{H}_{46}\text{N}_3\text{O}_8^+$ (calc. 696.3279).

Methyl pyridinium chloride [2]catenane 4Cl

A solution of **2Cl** (0.05 g, 0.048 mmol) and the calixdiquinone macrocycle **1** (0.06 g, 0.057 mmol) in DCM (25 mL) was degassed via a freeze-pump-thaw method. Under a nitrogen atmosphere, Grubbs' second generation catalyst (0.002 g, 0.0025 mmol, 5 mol.%) was added, and stirring was continued at room temperature overnight. To remove ruthenium and phosphine byproducts lead tetraacetate (0.002 g, 0.004 mmol) was then added and the mixture was stirred for a further night.³ The reaction mixture was filtered through a silica pad, the solvent was then removed *in vacuo* and the crude reaction mixture purified by silica gel preparative TLC (DCM:MeOH 92:8) to give the pure [2]catenane as a yellow solid (0.024 g, 0.014 mmol, 29%); ¹H NMR (500 MHz, CDCl₃) δ 9.75 (s, 1H), 9.16 (s, 1H), 9.05 (s, 2H), 8.68 (s, 2H), 8.61 (s, 2H), 8.25 (d, *J* = 7.9 Hz, 2H), 7.58 (t, *J* = 7.9 Hz, 1H), 6.78 – 6.64 (m, 16H), 6.22 (dd, *J* = 86.4, 9.0 Hz, 8H), 5.82 – 5.76 (m, 2H), 5.42 (s, 3H), 4.33 (d, *J* = 12.9 Hz, 4H), 4.08 – 3.90 (m, 16H), 3.90 – 3.79 (m, 8H), 3.79 – 3.71 (m, 4H), 3.71 – 3.63 (m, 4H), 3.57 – 3.41 (m, 4H), 3.06 (d, *J* = 12.9 Hz, 4H), 0.98 (s, 18H); ¹³C NMR (125 MHz, CDCl₃) δ 188.2, 185.4, 166.7, 159.9, 153.8, 152.9, 152.6, 152.5, 151.7, 148.9, 146.8, 144.7, 135.7, 133.4, 133.3, 132.4, 131.9, 129.4, 129.2, 125.5, 123.9, 116.0, 114.8, 114.7, 113.6, 73.7, 71.2, 68.7, 68.4, 67.4, 66.5, 65.2, 51.8, 41.4, 39.8, 34.1, 31.2, 30.2; *m/z* (ESI-HRMS) [M - Cl]⁺ 1644.7059, C₉₆H₁₀₂N₅O₂₀⁺ (calc. 1644.7113).

Benzyl pyridinium chloride [2]catenane 5Cl

A solution of **3Cl** (0.03 g, 0.041 mmol) and the calixdiquinone macrocycle **1** (0.05 g, 0.048 mmol) in DCM (25 mL) was degassed via a freeze-pump-thaw method. Under a nitrogen atmosphere, Grubbs' second generation catalyst (0.0017 g, 0.002 mmol, 5 mol.%) was added, and stirring was continued at room temperature overnight. To this lead tetraacetate (0.0014 g, 0.003 mmol) was then added and stirred for a further night. The reaction mixture was filtered through a silica pad, the solvent was then removed *in vacuo* and the crude reaction mixture was purified by silica gel preparative TLC (acetone:hexane 1:1) to give the pure [2]catenane as a yellow solid (0.023 g, 0.013 mmol, 27%); ¹H NMR (500 MHz, CDCl₃) δ 9.83 (s, 1H), 9.66 (s, 1H), 9.10 (s, 1H), 8.70 (s, 1H), 8.60 (s, 2H), 8.56 (s, 1H), 8.45 (s, 1H), 8.21 (d, *J* =

7.7 Hz, 2H), 7.96 (d, $J = 7.2$ Hz, 2H), 7.61 – 7.44 (m, 4H), 7.19 (s, 2H), 7.02 – 6.42 (m, 16H), 6.23 (dd, $J = 104.3$, 8.8 Hz, 8H), 5.97 – 5.74 (m, 2H), 4.89 (d, $J = 12.6$ Hz, 2H), 4.52 – 3.53 (m, 34H), 3.30 (d, $J = 10.0$ Hz, 4H), 3.20 (d, $J = 12.6$ Hz, 2H), 2.98 (d, $J = 12.6$ Hz, 2H), 1.01 (s, 18H); ^{13}C NMR (125 MHz, CDCl_3) δ 188.3, 187.9, 185.6, 183.1, 166.7, 160.5, 159.5, 153.8, 153.1, 152.7, 152.6, 151.3, 149.6, 147.5, 146.8, 145.8, 141.9, 136.1, 133.5, 133.3, 132.6, 132.5, 132.1, 131.8, 131.3, 130.5, 129.8, 129.7, 129.7, 129.4, 128.9, 128.8, 125.5, 124.3, 123.9, 116.1, 115.9, 114.9, 114.7, 113.4, 74.1, 71.4, 71.2, 68.9, 68.6, 68.0, 67.6, 66.5, 66.1, 65.5, 65.0, 41.3, 40.5, 39.3, 34.0, 31.2, 30.5, 29.9; m/z (ESI-HRMS) $[\text{M} - \text{Cl}]^+$ 1720.7492, $\text{C}_{102}\text{H}_{106}\text{N}_5\text{O}_{20}^+$ (calc. 1720.7426).

Anion exchange from 4Cl to 4PF₆

A solution of 4Cl (0.02 g, 0.012 mmol) in chloroform (2 mL) was repeatedly washed with 0.1 M NH_4PF_6 solution (10 x 1 mL) and water (10 x 1 mL). The solvent was then removed *in vacuo* and the residue was recrystallized from CHCl_3 :hexane to give the product as a yellow solid (0.017 g, 0.01 mmol, 85%); ^1H NMR (500 MHz, CD_2Cl_2 : CD_3CN 4:1) δ 9.01 (s, 1H), 8.57 (s, 2H), 8.52 (s, 1H), 8.01 (s, 2H), 7.98 (d, $J = 7.7$ Hz, 2H), 7.60 (t, $J = 7.7$ Hz, 1H), 7.35 (s, 2H), 6.89 (s, 4H), 6.87 (s, 4H), 6.72 – 6.57 (m, 8H), 6.37 (dd, $J = 70.8$, 8.8 Hz, 8H), 5.86 – 5.79 (m, 2H), 4.57 (s, 3H), 4.23 – 3.85 (m, 24H), 3.82 – 3.47 (m, 16H), 3.32 (d, $J = 12.1$ Hz, 4H), 1.10 (s, 18H); ^{19}F NMR (282 MHz, CD_2Cl_2 : CD_3CN 4:1) δ (ppm) - 72.4 (d, $J = 706$ Hz); m/z (ESI-MS) $[\text{M} - \text{PF}_6]^+$ 1644.70, $\text{C}_96\text{H}_{102}\text{N}_5\text{O}_{20}^+$ (calc. 1644.7113).

Anion exchange from 5Cl to 5PF₆

A solution of 5Cl (0.02 g, 0.011 mmol) in chloroform (2 mL) was repeatedly washed with 0.1 M NH_4PF_6 solution (10 x 1 mL) and water (10 x 1 mL). The solvent was then removed *in vacuo* and the residue was recrystallized from CHCl_3 :hexane to give the product as a yellow solid (0.015 g, 0.009 mmol, 80%); ^1H NMR (500 MHz, CD_2Cl_2 : CD_3CN 4:1) δ 9.08 (s, 1H), 8.97 (s, 2H), 8.15 (s, 1H), 7.94 (s, 2H), 7.77 (s, 2H), 7.75 (d, $J = 7.3$ Hz, 2H), 7.52 (t, $J = 7.3$ Hz, 1H), 7.49 – 7.36 (m, 3H), 7.22 (s, 2H), 6.76 (s, 4H), 6.73 (s, 4H), 6.62 – 6.27 (m, 18H), 5.84 (s, 2H), 4.35 – 3.44 (m, 40H), 3.20 (d, $J = 13.0$ Hz, 4H),

1.04 (s, 18H). ^{19}F NMR (282 MHz, $\text{CD}_2\text{Cl}_2:\text{CD}_3\text{CN}$ 4:1) δ (ppm) -73.1 (d, $J = 714$ Hz); m/z (ESI-MS) $[\text{M} - \text{PF}_6]^+$ 1720.72, $\text{C}_{102}\text{H}_{106}\text{N}_5\text{O}_{20}^+$ (calc. 1720.7426).

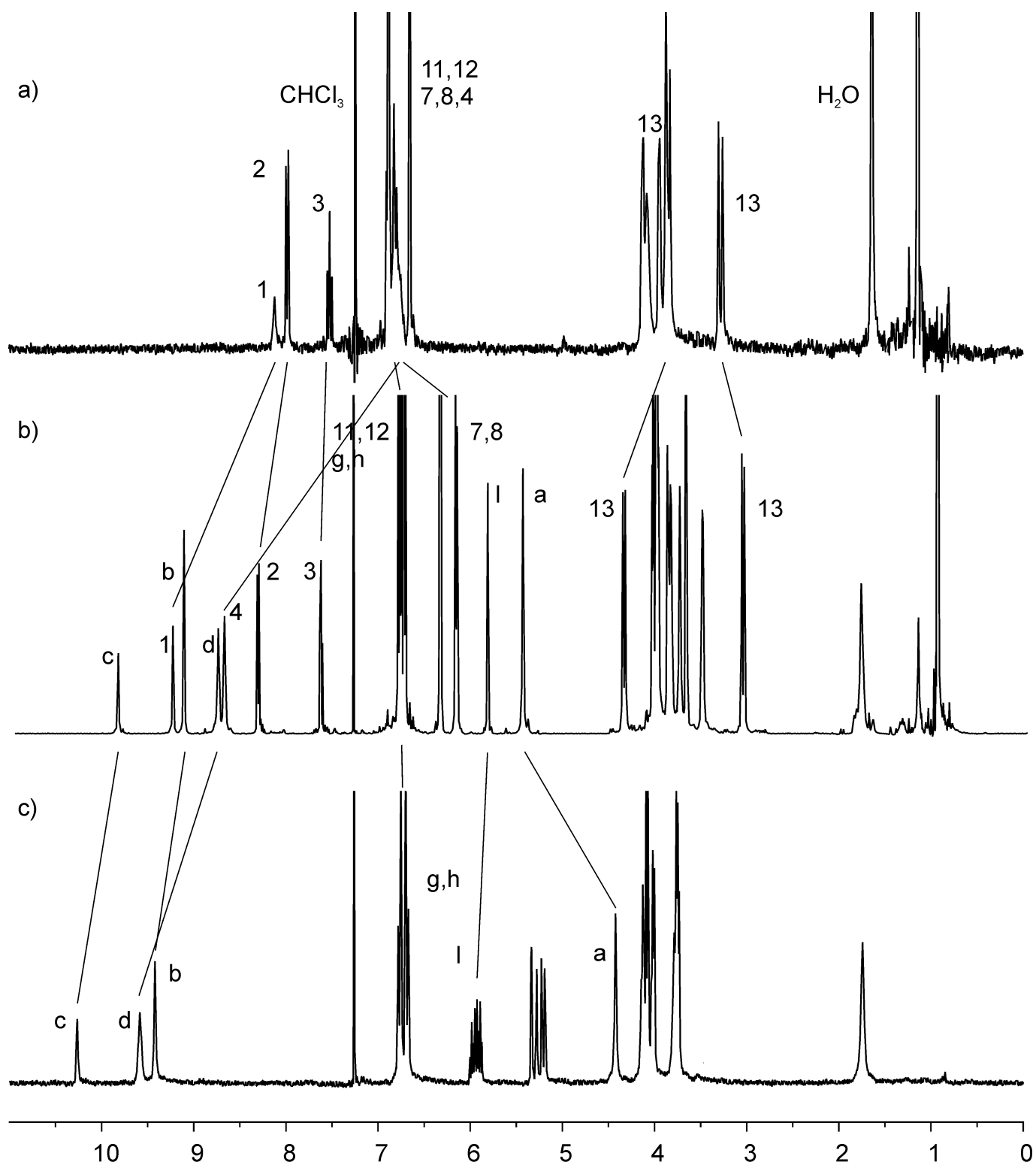


Figure S1 ^1H NMR spectra (300 MHz, CDCl_3 , 293 K) of a) calixdiquinone macrocycle **1** b) methyl [2]catenane **4Cl** and c) methyl pyridinium thread **2Cl**.

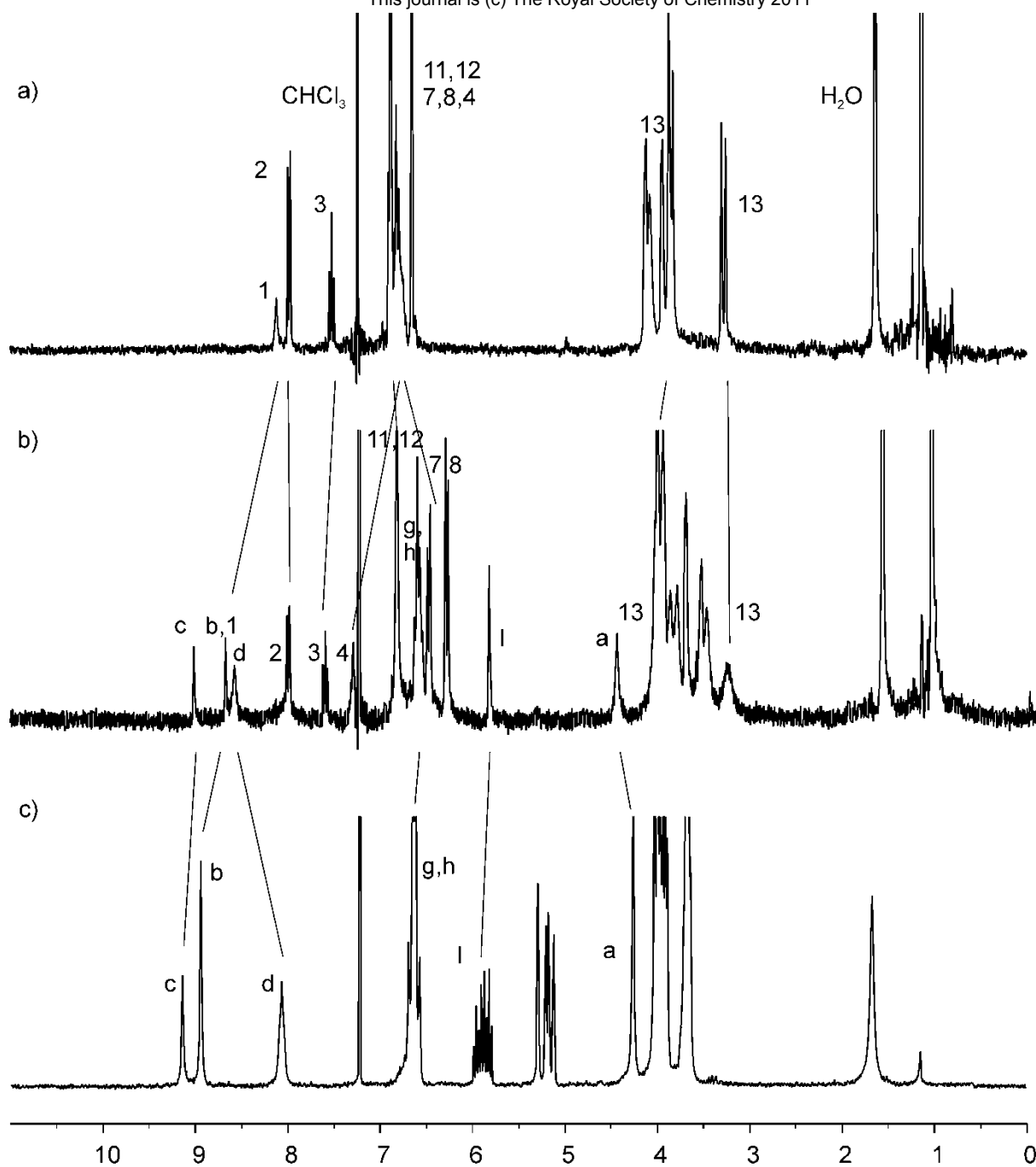


Figure S2 ^1H NMR spectra (300 MHz, CDCl_3 , 293 K) of a) calixdiquinone macrocycle **1** b) methyl [2]catenane **4** PF_6 and c) methyl pyridinium thread **2** PF_6 .

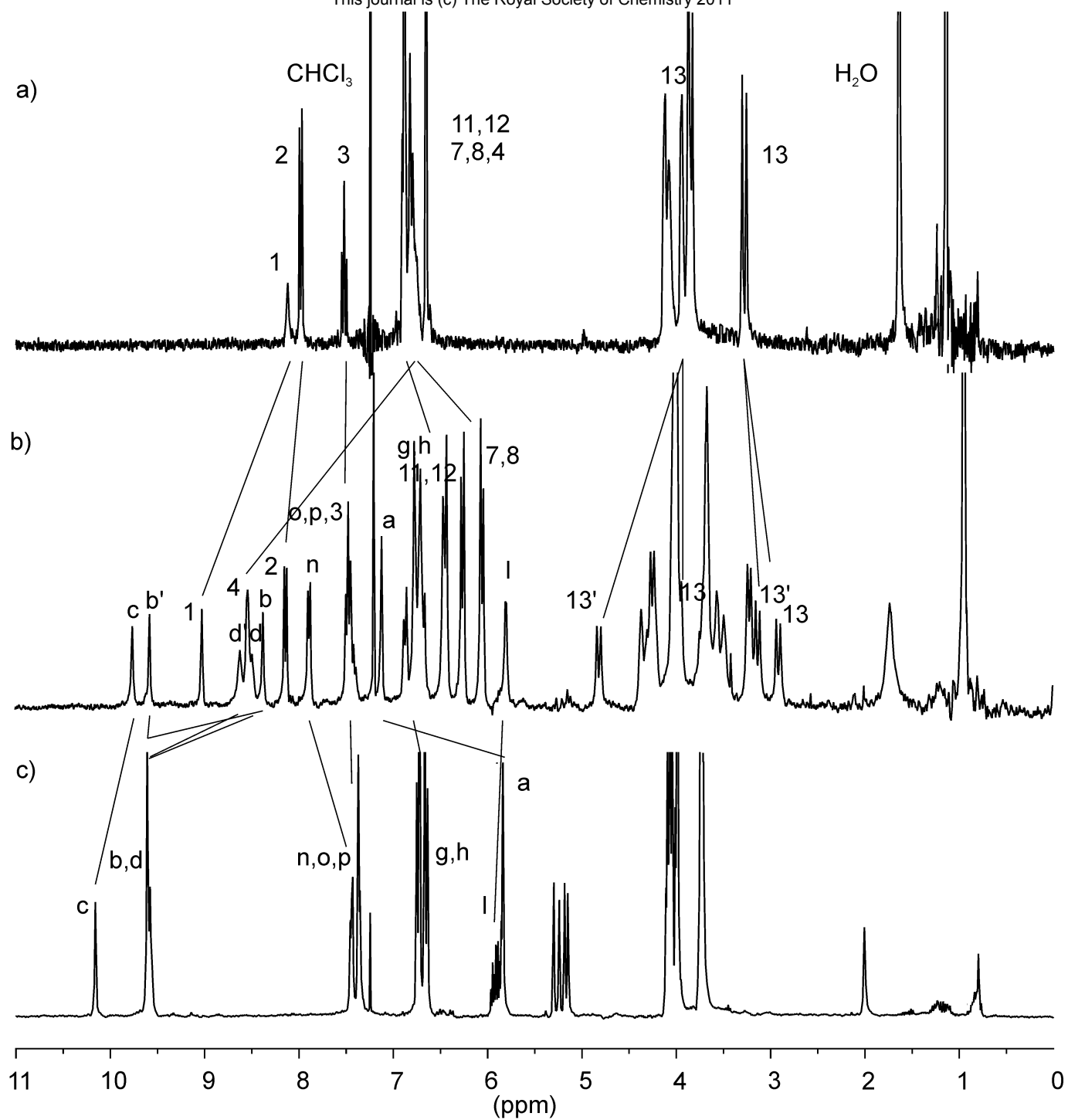


Figure S3 ^1H NMR spectra (300 MHz, CDCl_3 , 293 K) of a) calixdiquinone macrocycle **1** b) benzyl [2]catenane **5Cl** and c) benzyl pyridinium thread **3Cl**.

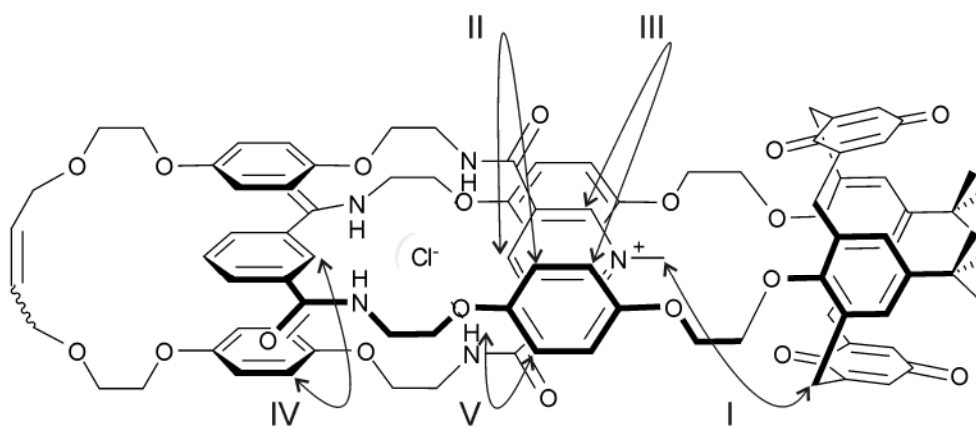
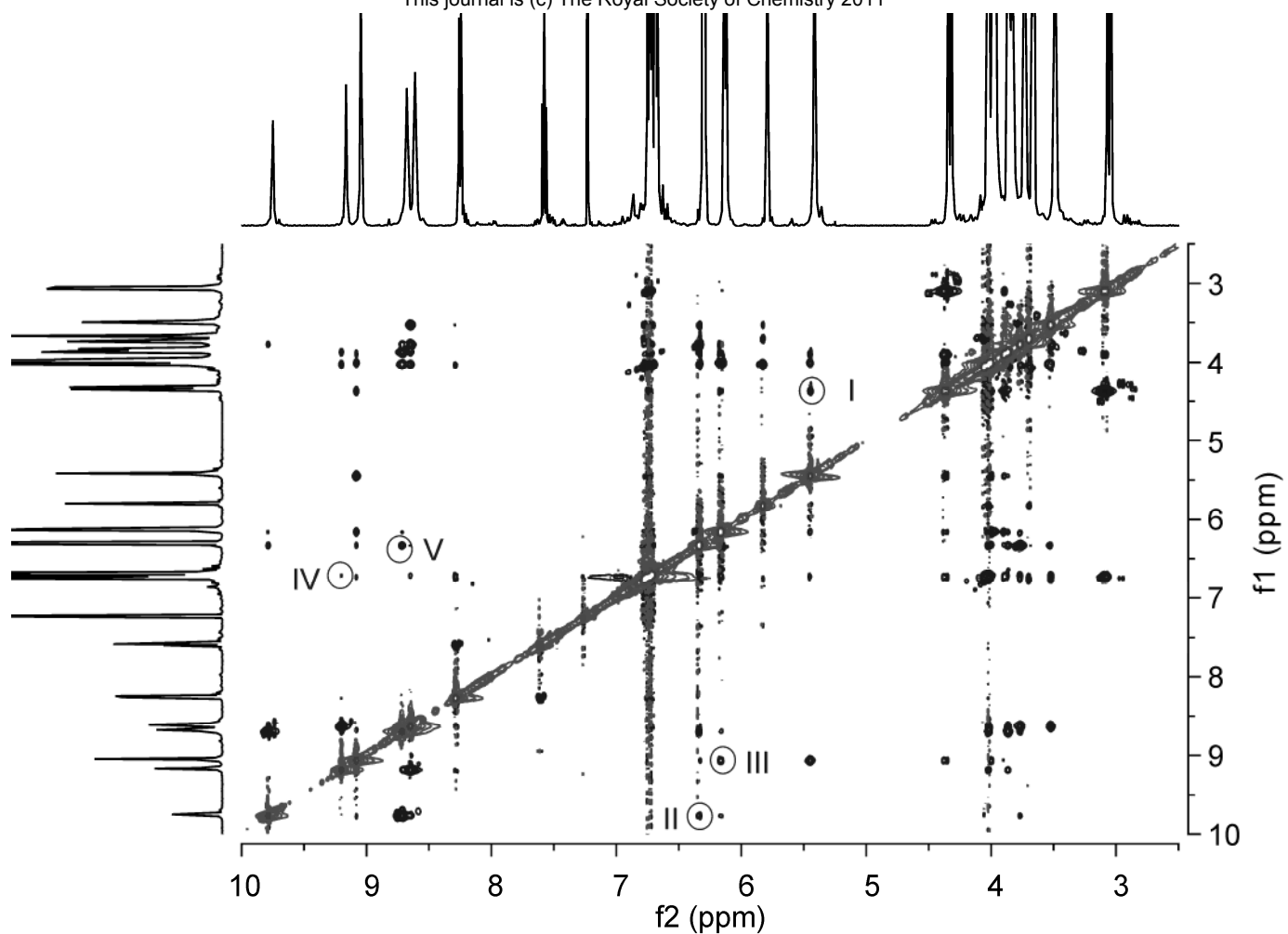


Figure S4 Partial ^1H - ^1H ROESY NMR spectrum (500 MHz, CDCl_3 , 293 K) of methyl [2]catenane **4Cl**.

Some of cross-couplings are shown in the schematic diagram below.

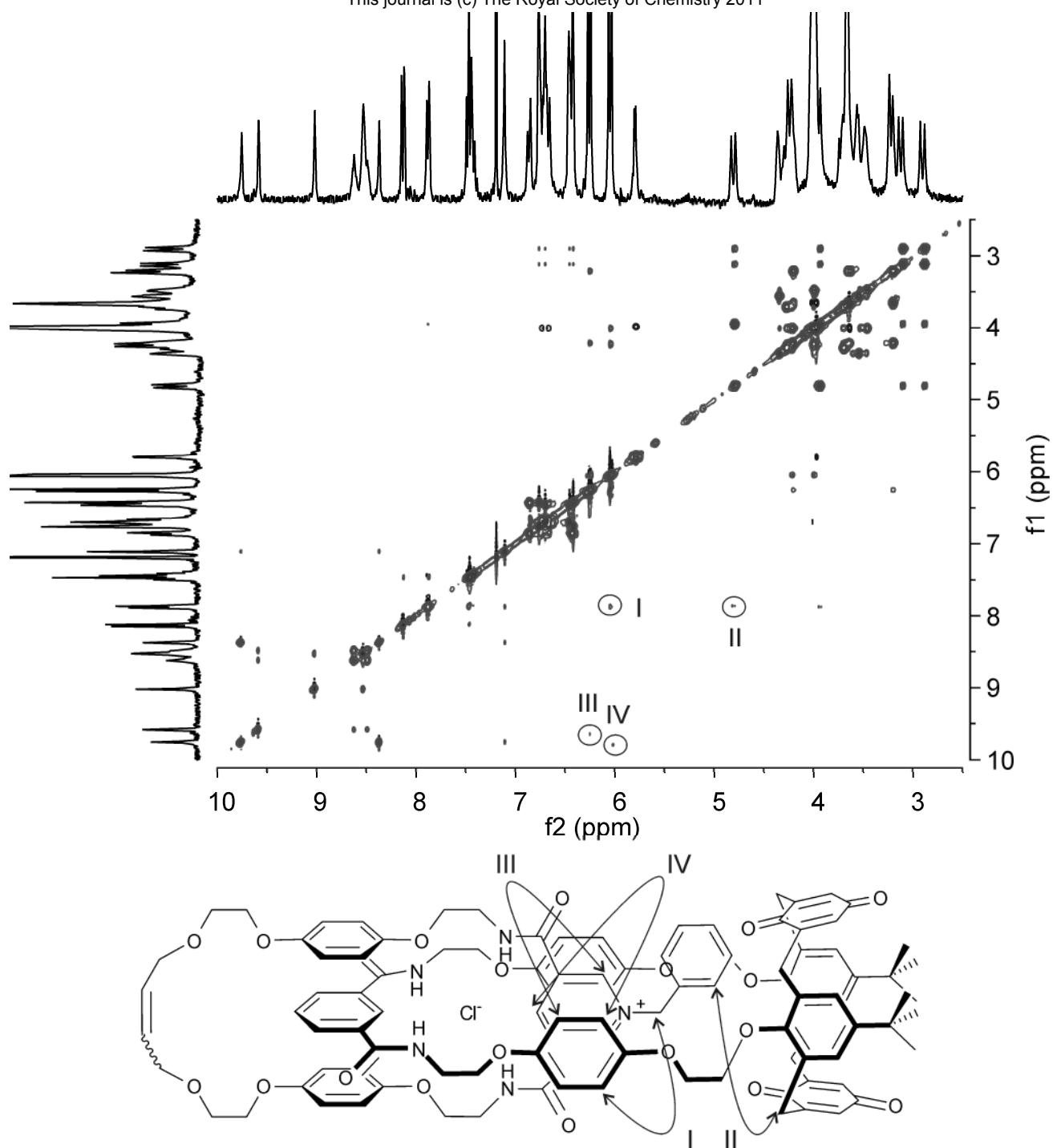


Figure S5 Partial ^1H - ^1H NOESY NMR spectrum (500 MHz, CDCl_3 , 293 K) of benzyl [2]catenane **5Cl**.

Some of cross-couplings are shown in the schematic diagram below.

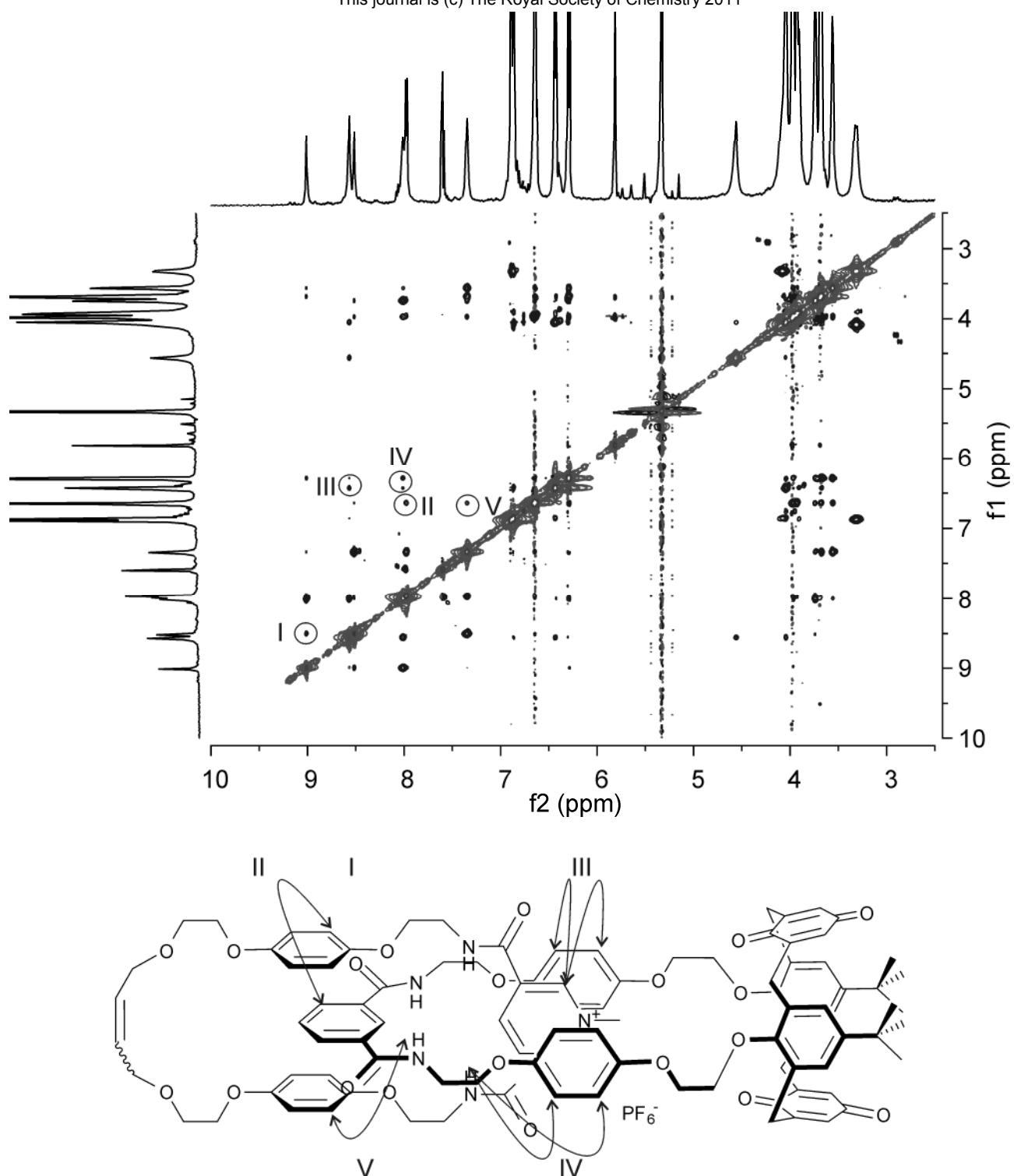


Figure S6 Partial ^1H - ^1H ROESY NMR spectrum (500 MHz, $\text{CD}_2\text{Cl}_2:\text{CD}_3\text{CN}$ 4:1, 293 K) of methyl [2]catenane 4PF_6 . Some of cross-couplings are shown in the schematic diagram below.

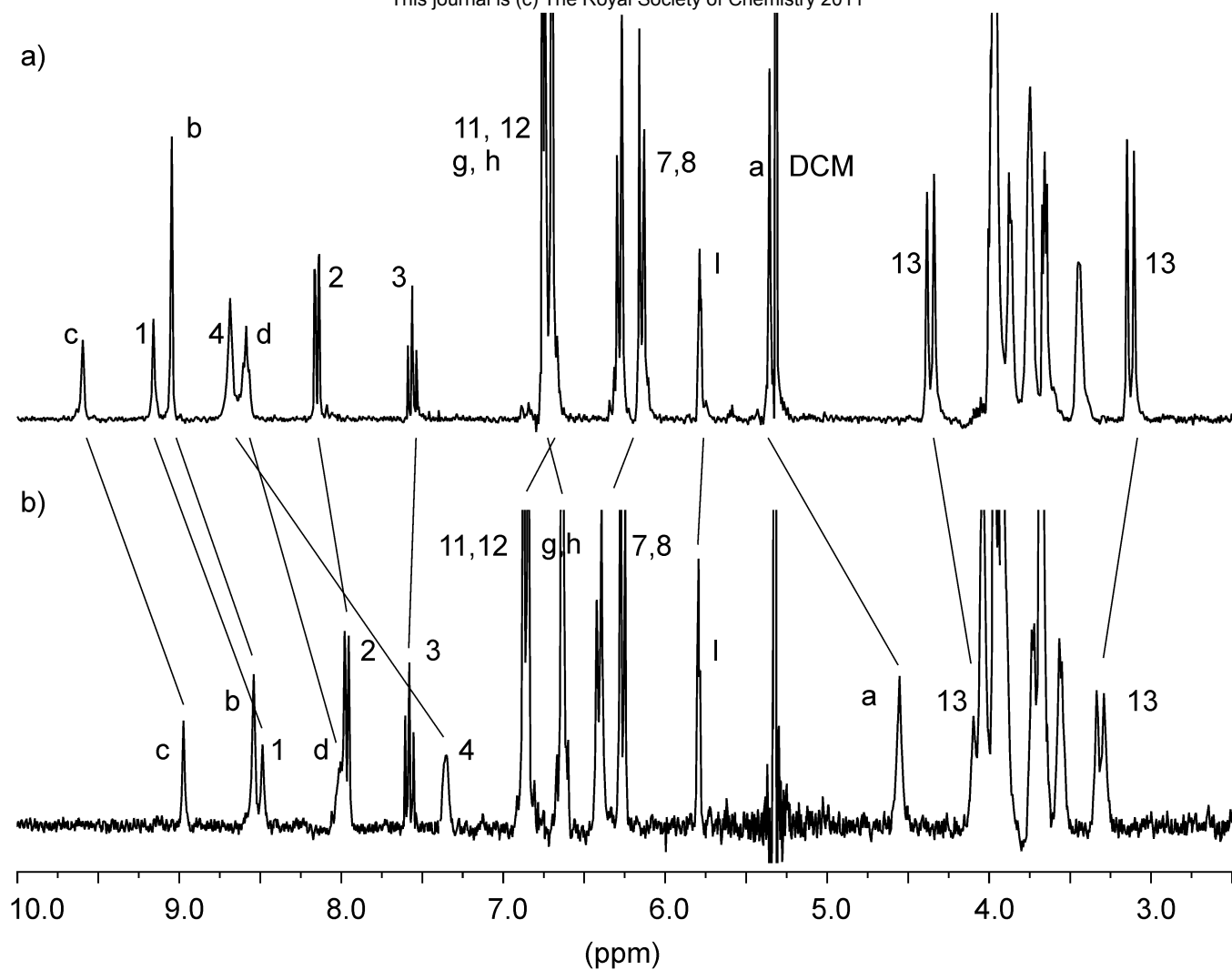


Figure S7 Partial ^1H NMR spectra (300 MHz, $\text{CD}_2\text{Cl}_2:\text{CD}_3\text{CN}$ 4:1, 293 K) of a) methyl [2]catenane **4Cl** and b) methyl [2]catenane **4PF₆**.

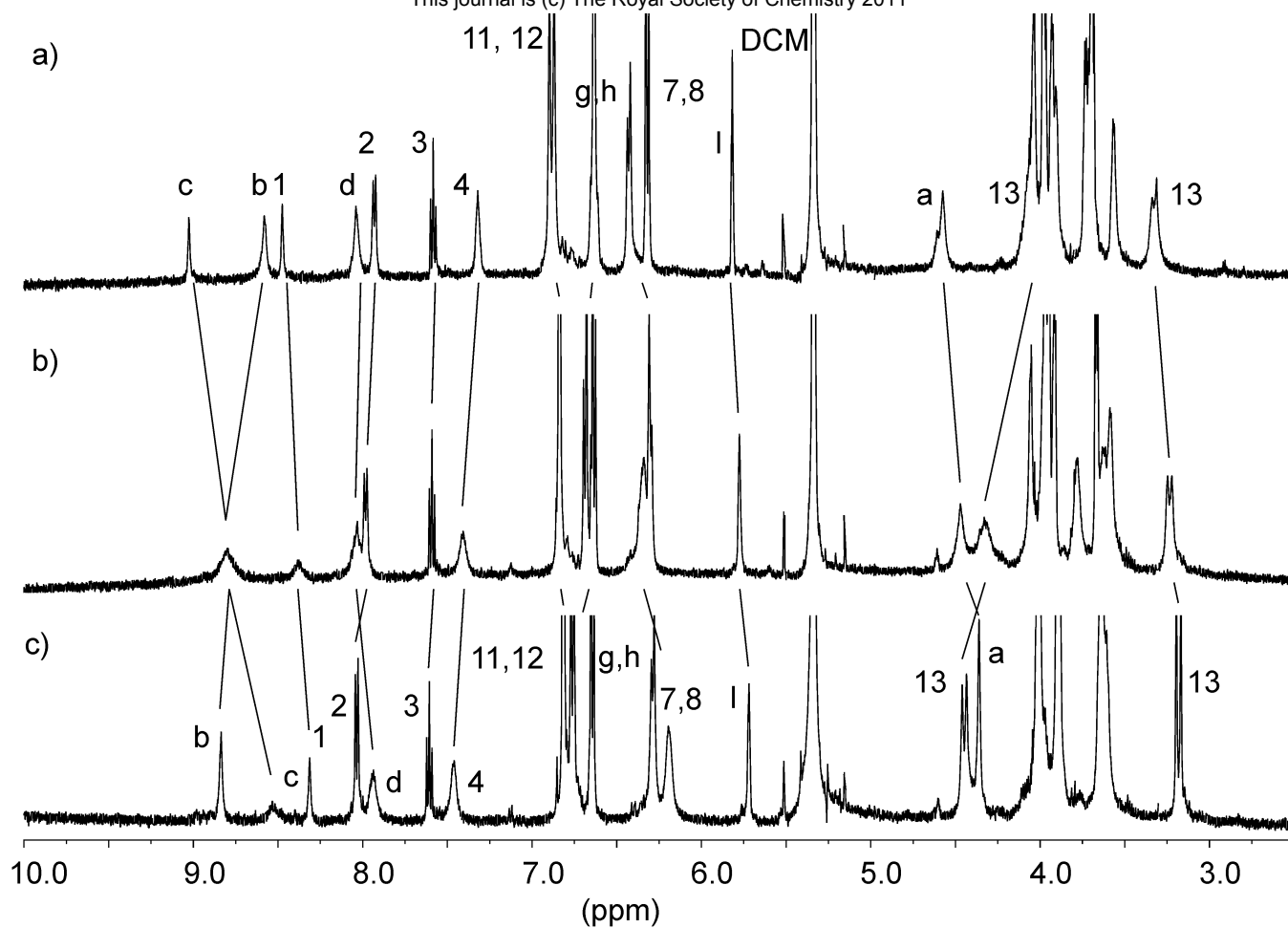


Figure S8 Partial ^1H NMR spectra (500 MHz, $\text{CD}_2\text{Cl}_2:\text{CD}_3\text{CN}$ 4:1, 293 K) of a) methyl [2]catenane 4PF_6 , b) 4PF_6 + 1 eq of NaClO_4 and c) 4PF_6 + 5 eq of NaClO_4 .

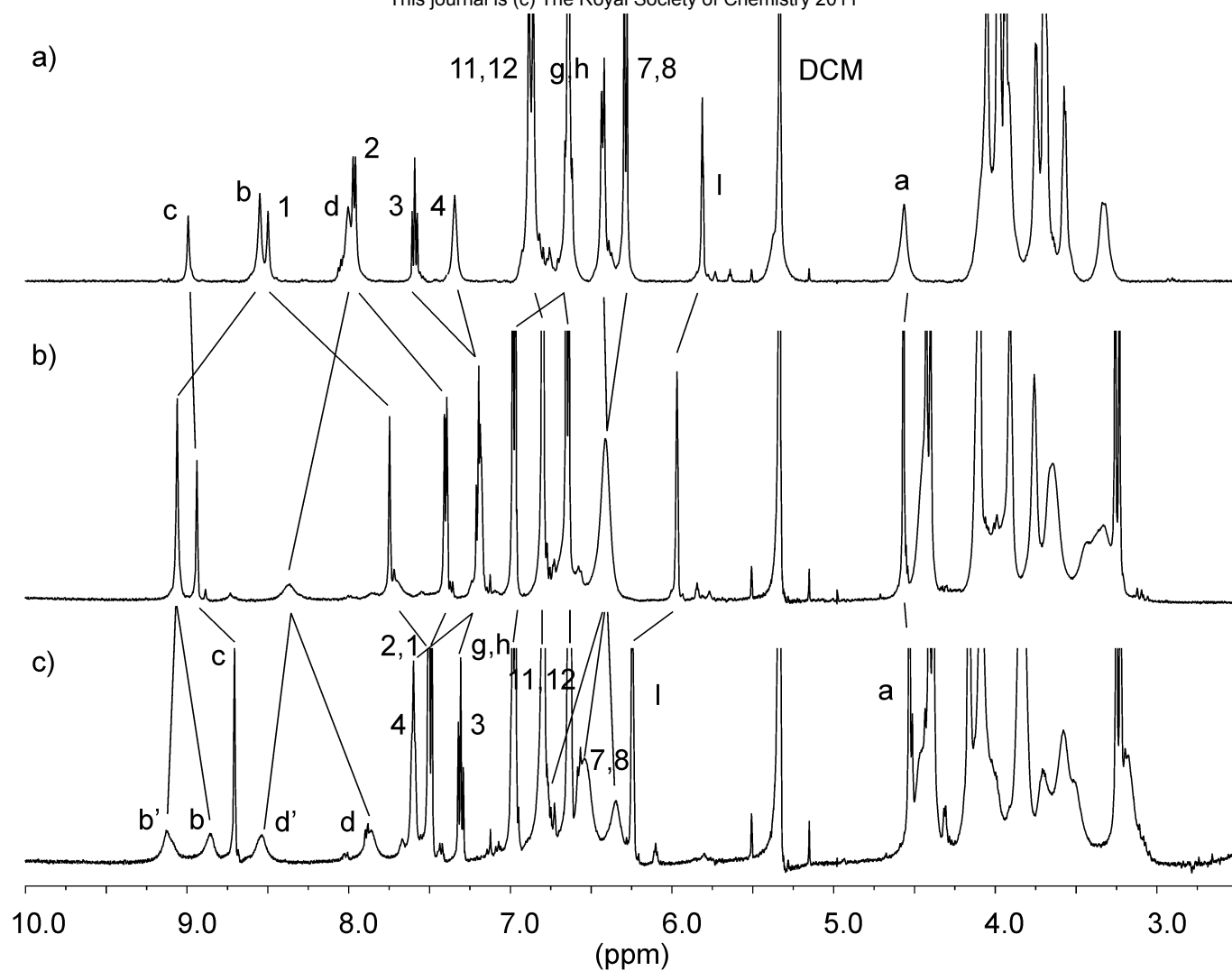


Figure S9 Partial ^1H NMR spectra (500 MHz, $\text{CD}_2\text{Cl}_2:\text{CD}_3\text{CN}$ 4:1, 293 K) of a) methyl [2]catenane 4PF_6 , b) $4\text{PF}_6 + 1$ eq of $\text{Ba}(\text{ClO}_4)_2$ and c) $4\text{PF}_6 + 5$ eq of $\text{Ba}(\text{ClO}_4)_2$.

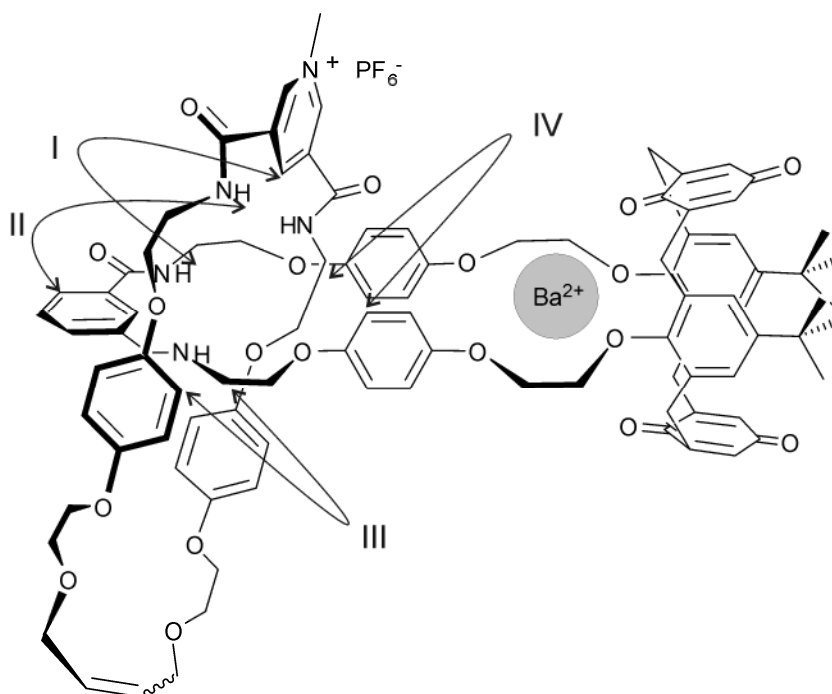
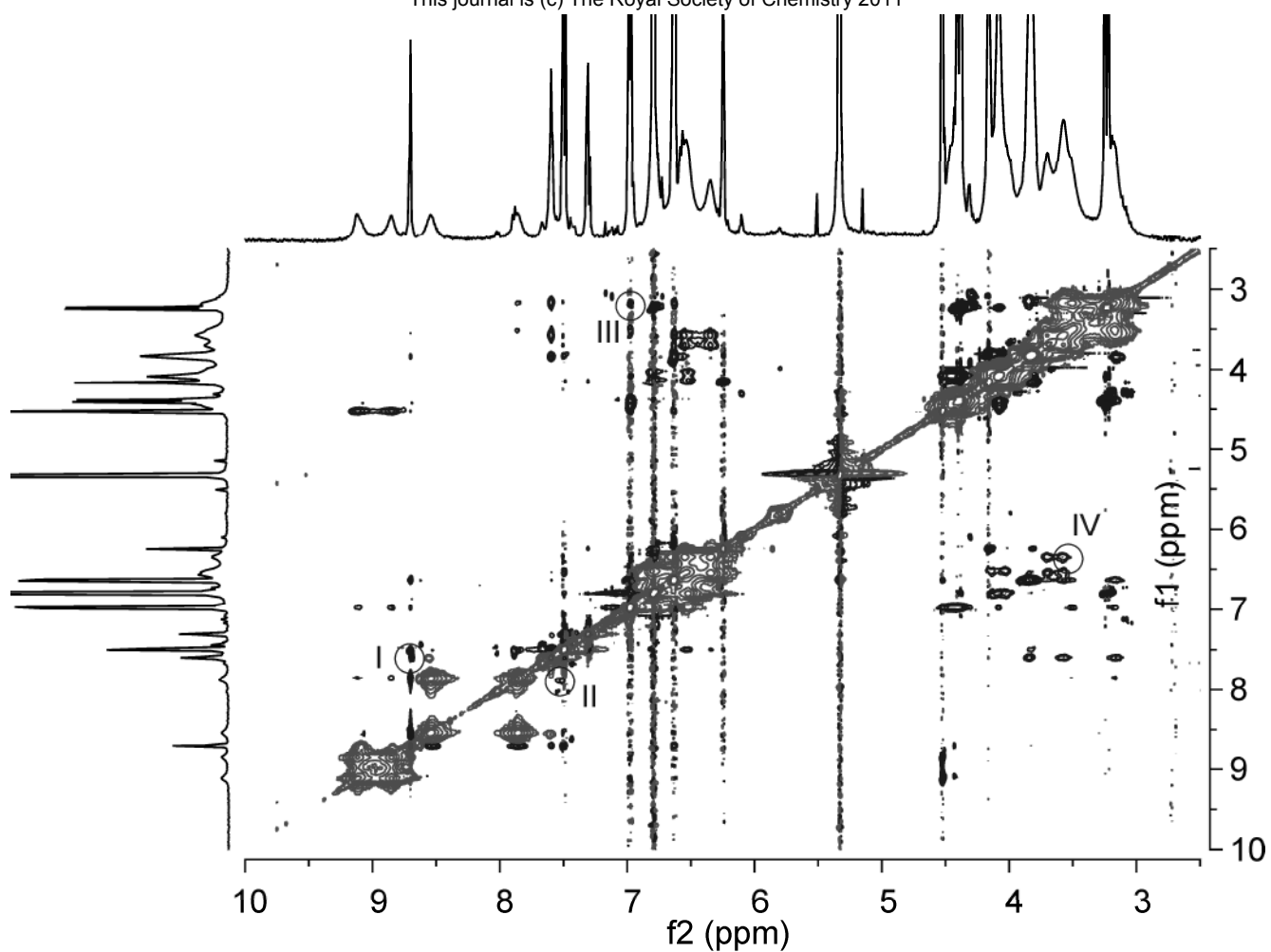


Figure S10 Partial 1H - 1H ROESY NMR spectrum (500 MHz, $CD_2Cl_2:CD_3CN$ 4:1, 293 K) of methyl [2]catenane $4PF_6 + 5eq$ of $Ba(ClO_4)_2$. Some of cross-couplings are shown in the schematic diagram below.

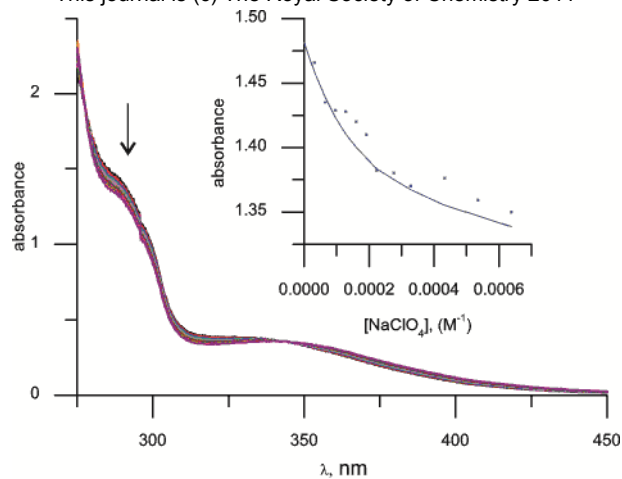


Figure S11 Change in a UV-vis spectrum of a 0.1 mM solution of the benzyl [2]catenane **5PF₆** in DCM:CH₃CN (4:1) solution on addition of NaClO₄ at 293 K. Inset: Change in the absorbance at 286 nm as a function of [NaClO₄] with calculated curve for log K_a = 4.17.

¹H NMR titration protocol

¹H NMR titration experiments were conducted on a Varian Unity Plus 500 spectrometer at 293 K. A solution of ionic guest (typically of 1 × 10⁻¹ mol/L concentration in CD₃CN) was added to a 0.6 mL solution of catenane **4PF₆** or **5PF₆** (typically 7 × 10⁻⁴ mol/L in CD₂Cl₂:CD₃CN (4:1)). Cation binding studies were performed using KPF₆, NH₄PF₆, NaClO₄ and Ba(ClO₄)₂. The chemical shifts of specific host protons (*a* or *l3*) were monitored for ten titration points (for 0, 0.25, 0.5, 0.75, 1.0, 1.5, 2.0, 3.0, 4.0 and 5.0 equivalents of added guest). Spectra were recorded after each addition, and the sample shaken thoroughly before measurement.

The resulting titration data were analyzed using the WinEQNMR computer program⁴ as the association of guest and host was fast on the NMR timescale (slowly exchange kinetic with Ba²⁺). In all cases the values of the observed chemical shift and guest concentration were entered for every titration point and estimates for the binding constant, limiting chemical shifts and complex stoichiometry were made. The various parameters were refined by non-linear least-squares analysis to achieve the best fit between observed and calculated chemical shifts; the program plots the observed shift versus the guest concentration, revealing the accuracy of the experimental data and the suitability of the model used. The input parameters were varied until the best-fit values of the stability constants, together with their errors,

converged. The values obtained are in general agreement with the association constants derived from the UV-vis spectroscopic titrations (Table S1) and show Na⁺ and K⁺ to be bound more strongly than the NH₄⁺ cation.

Table S1 Association constants log K_a for binding of NaClO₄, KPF₆ and NH₄PF₆ to catenane **4**PF₆ and catenane **5**PF₆ (500 MHz, CD₂Cl₂:CD₃CN (4:1), 293 K). Errors < 15%.

Cation	4 PF ₆ log K _a	5 PF ₆ log K _a
Na ⁺	3.43	3.46
K ⁺	3.62	3.34
NH ₄ ⁺	3.06	3.27

UV-vis titration protocol

UV-visible experiments were conducted on a PG T60 U spectrophotometer, at 293 K. A solution of guest (typically of 4 x 10⁻² mol/L concentration in CH₃CN) was added to a 3 mL solution of the host (typically 2 x 10⁻⁴ mol/L in CH₂Cl₂:CH₃CN (4:1)). Cation binding experiments were carried out using KPF₆, NH₄PF₆, NaClO₄ and Ba(ClO₄)₂. The absorption spectrum of the host molecule was monitored for thirteen titration points (for 0, 0.2, 0.4, 0.6, 0.8, 1.0, 1.5, 2.0, 2.5, 3.0, 3.5, 4.0 and 5.0 equivalents of added guest). Spectra were recorded after each addition (fast scan (0.4 nm), 250-600 nm), and the sample mixed thoroughly before each measurement.

The resulting titration data were analysed by the SPECFIT computer program⁵ to attempt binding constant determination. The spectra, together with the host and guest concentrations were entered into the program for every titration point and the complex stoichiometry and whether the component species were coloured was entered. The parameters are refined by global analysis that uses singular value decomposition and non-linear modeling by the Levenberg-Marquardt method. Using the calculated stability constants, the program plots the predicted spectra of the component species together with the observed and calculated absorption versus guest concentration at a given wavelength, both of which reveal the accuracy of the experimental data and the suitability of the model. The program also gives the

best-fit values of the stability constants together with their errors. The parameters were varied until the values for the stability constants converged.

Crystal structure data of calixdiquinone macrocycle 1

A single crystal X-ray structure was obtained by Dr. Christopher J. Serpell of the University of Oxford. Crystals were grown by slow evaporation of an acetonitrile:dichloromethane solution of macrocycle **1**. Single crystal X-ray diffraction data were collected using graphite monochromated Mo K α radiation ($\lambda = 0.71073 \text{ \AA}$) on a Nonius KappaCCD diffractometer. The diffractometer was equipped with a Cryostream N₂ open-flow cooling device,⁶ and the data were collected at 150(2) K. Series of ω -scans were performed in such a way as to cover a sphere of data to a maximum resolution of 0.77 \AA . Cell parameters and intensity data (including inter-frame scaling) were processed using the DENZO-SMN package.⁷ The structure was solved by direct methods using the SUPERFLIP software⁸ and refined using full-matrix least-squares on F² within the CRYSTALS suite.⁹

Non-hydrogen atoms were refined with anisotropic displacement parameters. Disorder in one of the *t*-butyl groups was observed, however attempts to resolve this disorder were unsatisfactory. A Slant Fourier map revealed that C(76) is best modeled as a single more diffuse ellipsoid. This is ascribed to the alignment of large rotational vibrations of the *t*-butyl group and “wagging” motion of the whole phenyl ring.

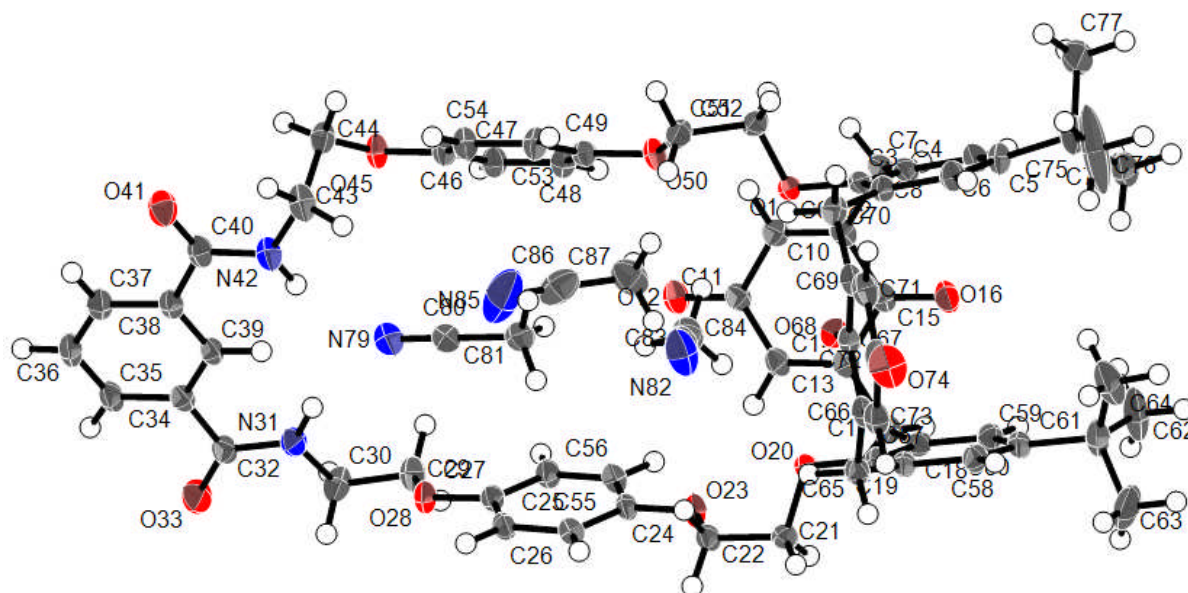


Figure S12 Thermal ellipsoid plot of calixdiquinone macrocycle **1** (created using CrystalMaker¹⁰).

Crystal structure data of benzyl [2]catenane **5Cl**

A single crystal X-ray structure was obtained by Nicholas G. White of the University of Oxford. Crystals were grown by slow evaporation of an acetonitrile:dichloromethane solution of benzyl [2]catenane **5Cl**. Single crystal X-ray diffraction data were collected using synchrotron radiation ($\lambda = 0.6889 \text{ \AA}$) on at Diamond Light Source, Beam I19. The diffractometer was equipped with a Cryostream N₂ open-flow cooling device,⁶ and the data were collected at 150(2) K. Series of ω -scans were performed in such a way as to collect a half-sphere of data to a maximum resolution of 0.77 \AA . Cell parameters and intensity data (including inter-frame scaling) were processed using the Rikagu Crystal Clear package.¹¹ The structure was solved by direct methods using SUPERFLIP⁸ and refined using full-matrix least-squares on F^2 within the CRYSTALS suite.⁹ Non-hydrogen atoms were refined with anisotropic displacement parameters. Except for water protons, hydrogen atoms were visible in the difference map and their positions and displacement parameters were refined using restraints prior to inclusion into the model using riding constraints.

There are a total of six hydrogen bonds involving the chloride anion. Four are from amide N-H groups ($\text{N-H}\cdots\text{Cl} = 3.328(4) - 3.570(5) \text{ \AA}$, $\angle\text{N-H}\cdots\text{Cl} = 157.3 - 171.4^\circ$), with a further bond from the *para*-pyridinium C-H ($\text{C-H}\cdots\text{Cl} = 3.467(6) \text{ \AA}$, $\angle\text{C-H}\cdots\text{Cl} = 174.0^\circ$) and a water solvate ($\text{O-H}\cdots\text{Cl} = 3.220(5) \text{ \AA}$,

$\angle \text{O-H}\dots\text{Cl} = 178.2^\circ$). Strong charge-assisted π - π stacking is observed between the pyridinium ring and the two hydroquinone rings (Centroid...centroid distances = 3.558 and 3.733 Å).

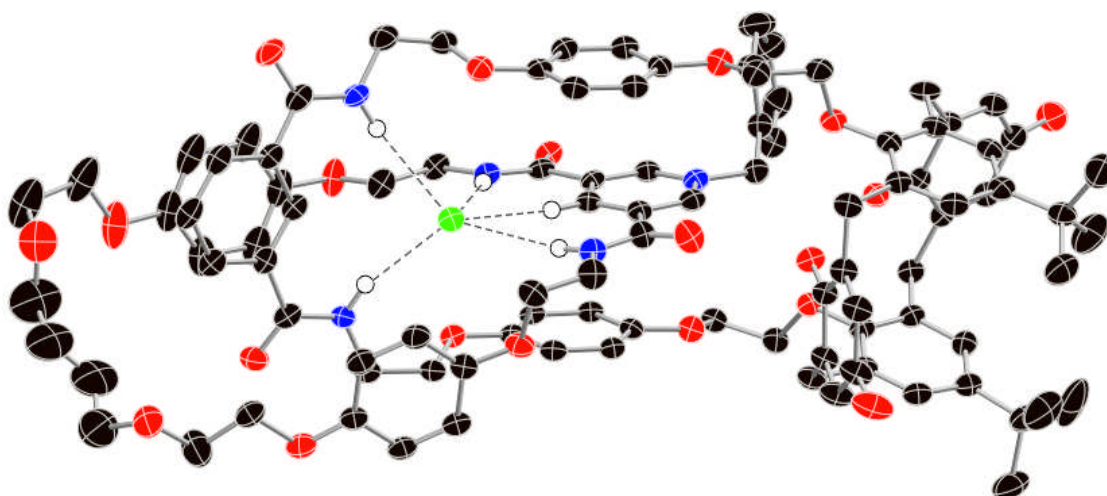


Figure S13 View of the benzyl [2]catenane **5Cl**. Thermal ellipsoids are shown at 30% probability level; hydrogen atoms (except those involved in hydrogen-bonding to the chloride anion) and water solvent molecules are omitted for clarity. Hydrogen bonds are shown as dashed lines.

Crystal structure data of methyl [2]catenane **4Cl**

A single crystal X-ray structure was obtained by Dr. Christopher J. Serpell of the University of Oxford. Crystals were grown by slow evaporation of an acetonitrile:dichloromethane solution of benzyl [2]catenane **4Cl**. Single crystal X-ray diffraction data were collected using synchrotron radiation ($\lambda = 0.6889$ Å) on at Diamond Light Source, Beam I19. The diffractometer was equipped with a Cryostream N_2 open-flow cooling device,⁶ and the data were collected at 150(2) K. Series of ω -scans were performed in such a way as to collect a half-sphere of data to a maximum resolution of 0.77 Å. Cell parameters and intensity data (including inter-frame scaling) were processed using the Rikagu Crystal Clear package.¹² The structure was solved by charge-flipping using SUPERFLIP,⁸ the output of which was a structure in the spacegroup P1. Refinement was conducted using full-matrix least-squares on F^2 within the CRYSTALS suite.⁹ After iterative Fourier cycles the full structure of the catenane was established, revealing two crystallographically independent interlocked molecules. Since the crystallisation of non-chiral species in P1 is extremely usual, attempts were made to collapse the structure into P-1. However,

despite the presence of an inversion centre appearing likely by visual inspection, this was unsuccessful. Close examination of the two structures reveals that the polyether portion of the pyridinium macrocycle is differently structured and that the proximal isophthalamide group of the calixquinone macrocycle is correspondingly displaced to fit this chain, resulting in a slight rotation of the two macrocycles with respect to each other (Fig. S13). Additionally, attempting to model these possibilities using partial occupancies in P-1 did not yield a stable refinement. While we recognise that P1 is still a very unlikely spacegroup for a non-chiral molecule, and that the structure presented is unsatisfactory in terms of parameters:data ratio and Flack parameter precision, in this case P1 appears to provide the best fit for the data. These problems notwithstanding, the connectivity and gross conformation of the catenane are not in doubt.

Twining was detected using Rotax, and the element scales were refined. Due to the low resolution of the data, bond lengths and angles lacked accuracy. This was accounted for by use of the MOGUL tool in CRYSTALS to add restraints to any unlikely geometric parameters. Additionally, restraints were added to the thermal parameters (anisotropic on all non-hydrogen atoms) to ensure a physically reasonable model. Hydrogen atoms were located geometrically, and then refined against the data, after which their locations were constrained using rides.

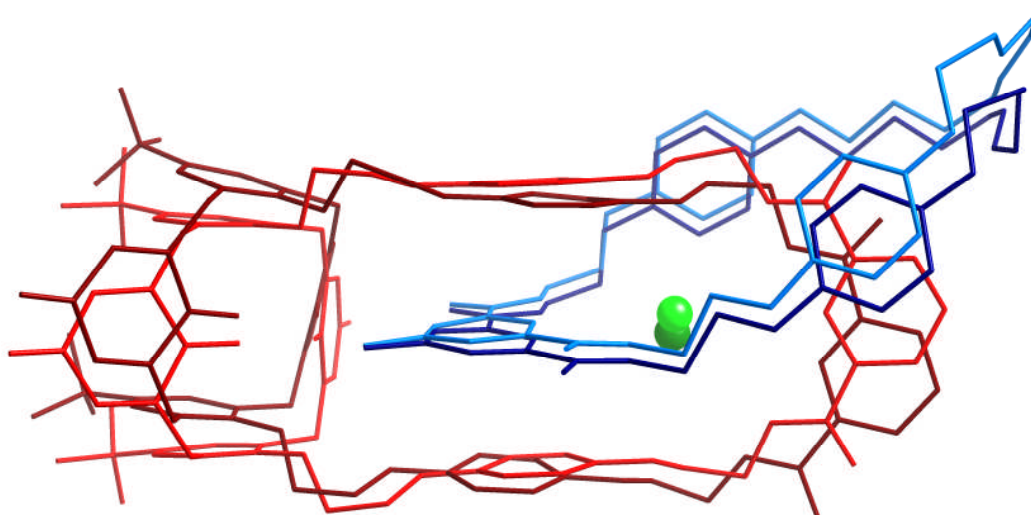


Figure S14 View of the methyl [2]catenane **4Cl**. Overlaying the two crystallographically independent catenanes (designated by darker and lighter colouration). Note the change in conformation of the rear polyether chain (top right), and the concomittant rotation of the calixquinone isophthalamide unit.

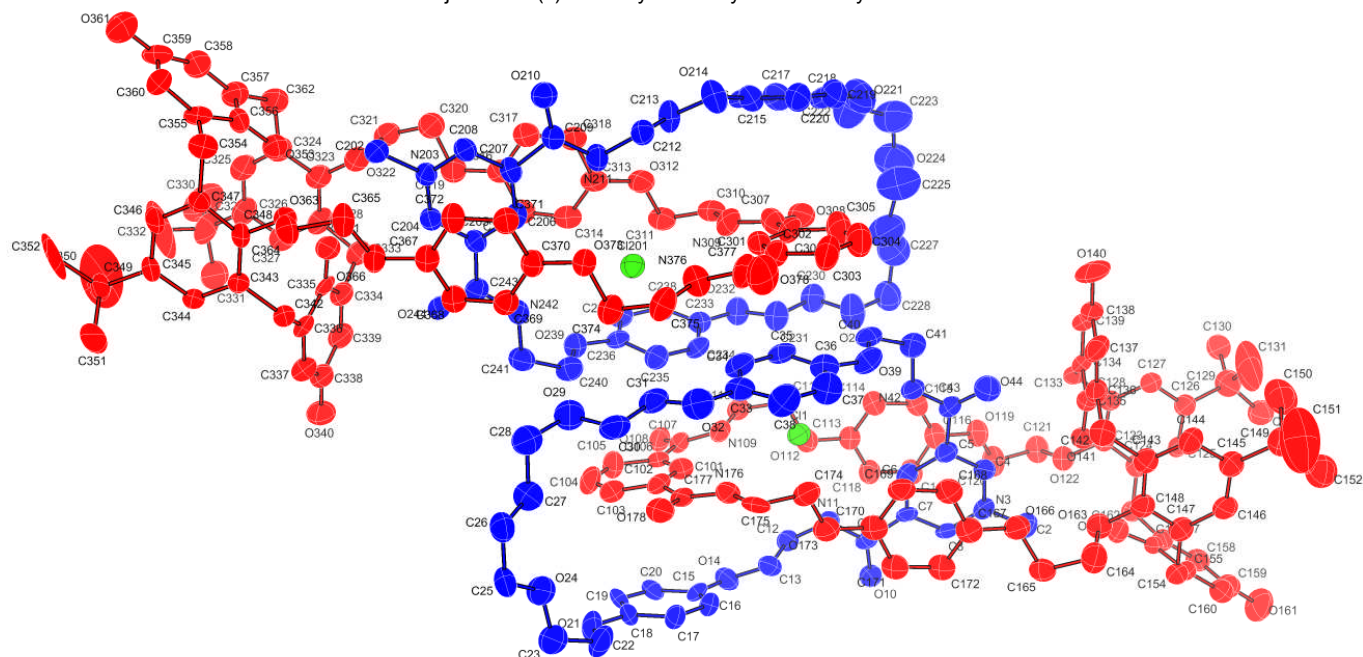


Figure S15 View of the methyl [2]catenane **4Cl**. Thermal ellipsoids are shown at 50% probability level; hydrogen atoms are omitted for clarity.

Table S2 Selected crystallographic data

Compound reference	1	4Cl	5Cl
Chemical formula	$C_{64}H_{64}N_2O_{12} \cdot 3(C_2H_3N)$	$C_{64}H_{64}N_2O_{12} \cdot C_{32}H_{38}N_3O_8 \cdot Cl$	$C_{64}H_{64}N_2O_{12} \cdot C_{38}H_{42}N_3O_8 \cdot 2(H_2O) \cdot Cl$
Formula Mass	1176.38	1681.35	1793.47
Crystal system	Triclinic	Triclinic	Monoclinic
$a/\text{\AA}$	11.58150(10)	11.009(7)	12.2168(13)
$b/\text{\AA}$	11.82310(10)	17.213(10)	24.953(3)
$c/\text{\AA}$	25.3961(3)	25.060(16)	31.028(3)
$\alpha/^\circ$	80.0523(4)	73.30(2)	90
$\beta/^\circ$	87.1768(4)	82.60(3)	97.6220(10)
$\gamma/^\circ$	66.4893(5)	79.77(3)	90
Unit cell volume/ \AA^3	3140.10(5)	4461(5)	9375.1(17)
Temperature/K	150	150	150
Space group	$P1$	$P1$	$P21/c$
No. of formula units per unit cell, Z	2	2	4
No. of reflections measured	32129	56767	107830
No. of independent reflections	13807	40992	30792
R_{int}	0.028	0.111	0.149
Final R_I values ($I > 2\sigma(I)$)	0.0502	0.1200	0.0971
Final $wR(F^2)$ values ($I > 2\sigma(I)$)	0.1151	0.3229	0.1680
Final R_I values (all data)	0.0646	0.1273	0.1268
Final $wR(F^2)$ values (all data)	0.1259	0.3295	0.1927

References

- 1 a) M. D. Lankshear, N. H. Evans, S. R. Bayly and P. D. Beer, *Chem. Eur. J.* **2007**, *13*, 3861-3870; b) J. A. Wisner, P. D. Beer, M. G. B. Drew and M. R. Sambrook, *J. Am. Chem. Soc.* **2002**, *124*, 12469-12476.
- 2 A. V. Leontiev, C. Jemmett and P. D. Beer, *Chem. Eur. J.* **2011**, *17*, 816-825.
- 3 L. A. Paquette, J. D. Schloss, I. Efremov, F. Fabris, F. Gallou, J. Mendez-Andino and J. Yang, *Org. Lett.* **2000**, *2*, 1259-1261.
- 4 M. J. Hynes, *J. Chem. Soc., Dalton Trans.* **1993**, 311-312.
- 5 *SPECFIT v. 2.02*, Spectrum Software Associates, Chapel Hill, NC.
- 6 Cosier, J.; Glazer, A. M. *J. Appl. Cryst.* **1986**, *19*, 105-107.
- 7 Z. Otwinowski, W. Minor, *Processing of X-ray Diffraction Data Collected in Oscillation Mode*; Academic Press, 1997.
- 8 L. Palatinus, G. Chapuis, *J. Appl. Cryst.* **1997**, *40*, 786-790.
- 9 P. W. Betteridge, J. R. Carruthers, R. I. Cooper, K. Prout, D. J. Watkin, *J. Appl. Cryst.* **2003**, 1487.
- 10 *CrystalMaker*, 2005, CrystalMaker Software Limited, Yarnton England.
- 11 CrystalClear: An Integrated Program for the Collection and Processing of Area Detector Data, Rigaku Corporation, 1997-2002.
- 12 CrystalClear: An Integrated Program for the Collection and Processing of Area Detector Data, Rigaku Corporation, 1997-2002.